

Graphene: Materially Better Carbon

Michael S. Führer, Chun Ning Lau,
and Allan H. MacDonald

Abstract

Graphene, a single atom-thick plane of carbon atoms arranged in a honeycomb lattice, has captivated the attention of physicists, materials scientists, and engineers alike over the five years following its experimental isolation. Graphene is a fundamentally new type of electronic material whose electrons are strictly confined to a two-dimensional plane and exhibit properties akin to those of ultrarelativistic particles. Graphene's two-dimensional form suggests compatibility with conventional wafer processing technology. Extraordinary physical properties, including exceedingly high charge carrier mobility, current-carrying capacity, mechanical strength, and thermal conductivity, make it an enticing candidate for new electronic technologies both within and beyond complementary metal oxide semiconductors (CMOS). Immediate graphene applications include high-speed analog electronics and highly conductive, flexible, transparent thin films for displays and optoelectronics. Currently, much graphene research is focused on generating and tuning a bandgap and on novel device structures that exploit graphene's extraordinary electrical, optical, and mechanical properties.

Introduction

Graphene, a single atom-thick plane of carbon atoms arranged in a honeycomb lattice, is the conceptual building block for many carbon allotropes, from three-dimensional graphite (a stack of graphene sheets), to one-dimensional carbon nanotubes (seamless graphene cylinders, see articles by Avouris and Martel and Liu and Hersam in this issue), to zero-dimensional buckyballs (closed graphitic cages). Until recently, this purely two-dimensional form of carbon existed only within three-dimensional graphite or tightly bound to another solid surface. Surface scientists had long been familiar with the latter appearance of graphene, or "monolayer graphite," as an undesirable impurity layer on metal or semiconductor surfaces.¹ However, the presence of a metal surface or of strong interactions between the host surface and monolayer graphite made electronic transport experiments difficult or impossible in most cases, and monolayer graphite remained an obscure curiosity.

In a seminal paper in 2004, Andre Geim and Kostya Novoselov at Manchester University reported that graphene could be obtained by simply rubbing a piece of crystalline graphite against almost any smooth

surface, a process referred to as mechanical exfoliation.^{2,3} After exfoliating graphene on thin silicon dioxide over silicon, they found that single graphene layers could be readily identified in an optical microscope, and that they display strong field-effect transistor (FET) behavior, with silicon acting as the gate. Soon Geim and Novoselov, and simultaneously Philip Kim at Columbia University, demonstrated the quantum Hall effect in mechanically exfoliated graphene.^{4,5} The observation of the anomalous half-integer quantization of the Hall conductance⁶ provided convincing proof of the massless chiral nature of charge carriers in graphene (see the following subsection *Massless Charge Carriers*). Additionally, the occurrence of the quantum Hall effect, previously observed only in the highest-quality semiconductor heterostructures, in a material fabricated by such a pedestrian technique, sparked a firestorm of interest that continues to this day.

In parallel with the efforts of Geim and Novoselov, other researchers were independently pursuing the preparation of graphene on metal and semiconductor surfaces. Walter de Heer and Phillip First of Georgia Tech pioneered the electronic characterization of graphene on silicon

carbide,⁷ which is emerging as a promising material for electronics applications, and is the subject of the review by First and co-authors in this issue. Several researchers have recently revisited the growth of graphene on metal surfaces^{8–10} and have developed techniques to transfer graphene from metals to insulating surfaces where electronic measurements can be performed (see section on "Synthesis of Graphene").

The explosive growth of graphene research has been fueled, in part, by its extremely promising properties as an electronic material. Graphene has been shown to be an extraordinary conductor of electricity, with an intrinsic charge carrier mobility at room temperature of 200,000 cm²/Vs, higher than any other known material.^{11,12} A carrier mobility of up to 120,000 cm²/Vs has been achieved in suspended graphene samples at 240 K.¹³ The thermal conductivity of graphene is higher than that of diamond at room temperature,¹⁴ and graphene can sustain current densities of 5×10^8 A/cm², or about 1 μ A per atomic row of carbon.^{15,16} Although graphene does not have an intrinsic bandgap, a number of gap creation strategies have been proposed and are being explored. This material of superlatives is now a promising candidate for new electronic technologies, both within and beyond complementary metal oxide semiconductors (CMOS).

Why Graphene is Special *Massless Charge Carriers*

Graphene owes its amazing electronic properties to its honeycomb lattice carbon network, in which 2s, 2p_x, and 2p_y orbitals hybridize such that each carbon atom is bonded to its three neighbors by strong "sp²" or "sigma" bonds. The remaining p_z or "pi" orbital determines the low-energy electronic structure of graphene. The dispersion of the pi electrons in graphene was first calculated within the tight-binding approximation in 1947.¹⁷ The unit cell of graphene contains two pi orbitals, which disperse to form two pi bands that may be thought of as bonding (the lower energy valence band) and anti-bonding (the higher energy conduction band) in nature (see Figure 1). The bonding-anti-bonding gap closes at the corners of the Brillouin zone, or the K points. As a result, the pi-band dispersion is approximately linear around the K points: $E = \hbar v_F |k|$, where k is the wave vector measured from K, \hbar is Planck's constant h divided by 2π , and v_F is the Fermi velocity in graphene, approximately 10⁶ m/s.

A linear dispersion normally characterizes particles whose kinetic energy vastly

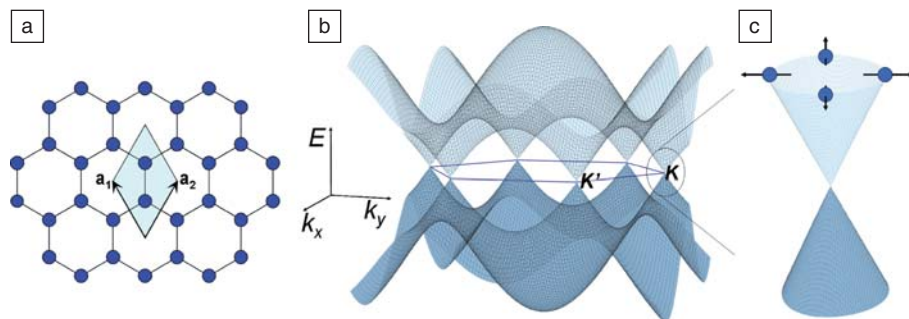


Figure 1. (a) Graphene honeycomb lattice with two atoms per unit cell and underlying triangular Bravais lattice with lattice vectors \mathbf{a}_1 and \mathbf{a}_2 . (b) Tight-binding band structure of graphene pi bands, considering only nearest-neighbor hopping. E is energy, and k_x and k_y are the x - and y -components of the wave vector. (c) Band structure near \mathbf{K} point showing the linear dispersion relation. The arrows denote the direction of the pseudospin vector.

exceeds their rest mass energy. Electrons in graphene thus behave like photons or other ultra-relativistic particles (such as neutrinos), with an energy-independent velocity v_F that is approximately 300 times smaller than the speed of light. However, the connection to relativistic physics is even deeper than this: the Hamiltonian describing particles near the \mathbf{K} point may be written as $H = v_F \boldsymbol{\sigma} \cdot \mathbf{p}$, where $\mathbf{p} = \hbar \mathbf{k}$ is the momentum vector measured from the \mathbf{K} point, and $\boldsymbol{\sigma}$ are Pauli spin matrices acting on the honeycomb sublattice degrees of freedom. This is the Dirac equation for massless relativistic particles. The positive energy conduction band and the negative energy valence band touch at the \mathbf{K} point, just as electron and positron bands touch at zero momentum in the zero mass limit of the relativistic Dirac equation. (For this reason, the Brillouin-zone corners in graphene are often referred to as Dirac points.) When the sublattice degree of freedom is viewed as an effective spin (a “pseudospin”), the pseudospin is parallel to momentum in the conduction band and antiparallel to momentum in the valence band. This correlation between momentum and pseudospin is precisely analogous to the correlation between momentum and real spin in the Dirac equation, which leads in the zero mass limit to the well-known helicity eigenstates.

High Mobility

The pseudospin of charge carriers has real consequences for graphene. In particular, backscattering of charge carriers is suppressed, because backscattering would involve reversing not only the momentum of the charge carrier, but also its pseudospin, which is forbidden for long-wavelength disorder. This fact has enormous consequences for charge carrier transport in one-dimensional carbon nanotubes, in which backscattering is the only

possibility.^{18,19} As a result, charge carriers can travel for microns in nanotubes at room temperature without scattering.^{20,21} In graphene, the absence of backscattering is a significant factor behind the high mobility observed in the material. Weak electron-acoustic-phonon coupling, high sound velocity, and the near-absence of point disorder in the graphene lattice in as-fabricated samples also contribute to graphene’s high mobility.

Truly 2D Material

The physics of two-dimensional electron systems has been studied since the mid-1960s, when Fowler et al.²² observed that the conductance of electrons near the Si/SiO₂ interface in a metal oxide semiconductor field-effect transistor (MOSFET) was periodic in inverse magnetic field strength, proving that motion perpendicular to the interface was quantized. Standards have now been raised by graphene sheets, in which two-dimensionality is achieved on an atomic length scale. One important consequence is that the size quantization energy scale in graphene is set by the difference in energy between pi and sigma orbitals, which is on the scale of electron volts instead of the meV scale typical of MOSFETs or quantum wells. Two-dimensionality in graphene is therefore much more robust: its electrons remain two-dimensional up to room temperature and beyond to the melting point of graphene. Because graphene electrons are more strongly bound to the graphene plane than semiconductor electrons are bound to a quantum well, chemical doping or electrostatic gating can induce and tune net carrier densities over a very large range (more than $\pm 10^{13} \text{ cm}^{-2}$, equivalent to Fermi energy shifts of $\pm 350 \text{ meV}$). Thus, graphene behaves like a two-dimensional metal even at room temperature—one

with widely tunable properties such as work function, density of states, conductivity, and more. With graphene, two-dimensional electron physics has emerged from low-temperature physics laboratories to join the room-temperature world.

Other Extraordinary Properties of Graphene

Graphene has a number of other exceptional properties. Because of its robust network of sp^2 bonds, graphene is the strongest material ever studied,²³ allowing, for example, one atom-thick graphene membranes that are impermeable to gas molecules to act like nano-balloons.²⁴ On the other hand, graphene is also incredibly supple, forming ripples when compressed and strained.^{25–27} This readiness to deform, combined with electrical properties that depend on local morphology,^{26–30} could be exploited for strain-based graphene electronics.³¹

Graphene’s thermal properties are equally extraordinary. Graphene has extremely high thermal conductivity, up to 5000 W/m K at room temperature,¹⁴ 20 times higher than that of copper, and can maintain better thermal contact with SiO₂ than other carbon materials.³² These findings are encouraging for potential applications in microelectronics and thermal management structures. Finally, graphene’s thermal expansion coefficient is large and *negative*, measured to be $\sim -6 \times 10^{-6} / \text{K}$,²⁵ which is 5–10 times larger than that in ordinary graphite. The large negative thermal expansion coefficient, which will be an important consideration in management of thermal stress in graphene devices, arises from the abundant out-of-plane phonons and is a direct consequence of the two-dimensionality of graphene.

Synthesis of Graphene

The most commonly adopted method of graphene production is mechanical exfoliation, that is, directly “rubbing” bulk graphite onto a smooth substrate.³ Mechanical exfoliation can reliably produce large area (up to 1 mm² has been reported—see Figure 2) graphene sheets with surprisingly good electrical properties; they routinely exhibit the quantum Hall effect^{4,5} and have low-temperature mobilities up to 20,000 cm²/Vs.

The success of the mechanical exfoliation technique relies on the surprising fact that the graphene layers can be located using an optical microscope. Although Raman spectroscopy can be used to determine the number of layers in a thin graphite sheet,³³ human eyes amazingly remain the fastest and most convenient

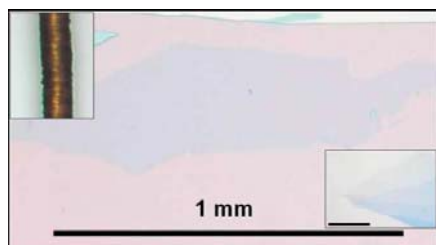


Figure 2. Optical image of a large single-layer graphene sheet (courtesy of W. Bao and C.N. Lau). Left inset: a hair of $\sim 100\ \mu\text{m}$ width shown on the same scale as the main panel. Right inset: Optical image of a graphene sheet with 1-, 2- and 3-layer-thick regions and a thicker (≥ 5 layers) region. Scale bar: $50\ \mu\text{m}$.

way to identify single- and bi-layer graphene. Novoselov and Geim used a silicon substrate with a 300-nm-thick layer of SiO_2 for their initial experiments.³ Under typical white light illumination, single-layer graphene on such a substrate appears as very pale purple and almost transparent, and bi-layer graphene appears slightly darker in color (see Figure 2). The thickness-dependent color arises from a combination of two factors: (1) the thin graphene layer adds to the optical path of the reflected light, thus resulting in interference between the paths that reflect off graphene and the substrate,³⁴ and (2) each graphene layer absorbs about 2.3% of light,^{35–37} due to the so-called “universal optical conductivity,” which is another direct consequence of graphene’s electronic structure.

The ease of graphene production by mechanical exfoliation has made the field of two-dimensional electron physics accessible to practically any investigator. However, this technique is tedious and produces randomly placed graphene sheets. Obviously, to realize graphene’s potential as a post-silicon electronic material, techniques for large-area synthesis of graphene are needed, prompting a return to the surface science techniques for growth of graphene on metal and semiconductor substrates. Epitaxial growth of graphene on silicon carbide (SiC) substrates has emerged as a particularly promising technique,^{7,38} as discussed in detail by First et al. in this issue. Very recently, there has also been significant progress in growing graphene on large-area polycrystalline metallic substrates, such as $\text{Ni}^{8,10}$ and Cu^9 via chemical vapor deposition. Typically, such synthesis is performed by placing the metal substrate in a furnace in a methane/hydrogen mixture at 1000°C . Single-layer graphene

covering up to 95% of the surface area can be obtained.⁹ To fabricate devices, graphene can be transferred by polydimethylsiloxane stamps or by dissolving the underlying metallic substrate in a metal etchant and “scooping” the single-layer graphene up with desired substrates (e.g., Si/SiO_2). Quantum Hall effect and low-temperature mobilities up to $3700\ \text{cm}^2/\text{Vs}$ have been observed in these metal-grown graphene sheets.⁸ Although still in its infancy, recent progress on epitaxial growth represents an important step toward the development of large-scale graphene-based electronic devices.

Graphene Electronics Gapless Analog Devices

The first-observed and still most-examined aspect of graphene is its ambipolar FET behavior, in which a gate electrode can change both the charge carrier density and type (n or p). Figure 3a shows the conductivity as a function of gate voltage $\sigma(V_g)$ at a temperature of 2.1 K for an exfoliated graphene device on a SiO_2/Si substrate, with the heavily doped Si acting as the gate.³⁹ The conductivity $\sigma(V_g)$ shows a characteristic “V” shape, with the minimum conductivity occurring at a gate voltage $V_{g,\text{min}}$ that corresponds closely to the point of charge neutrality, as deter-

mined from the Hall effect. For $V_g < V_{g,\text{min}}$ graphene is p -type (current is carried by holes in the valence band), and for $V_g > V_{g,\text{min}}$ graphene is n -type (current is carried by electrons in the conduction band). The conductivity $\sigma(V_g)$ is nearly electron-hole symmetric, reflecting the symmetric band structure (see Figure 1). At high carrier concentration (i.e., far from $V_{g,\text{min}}$), $\sigma(V_g)$ is roughly linear, indicating a nearly constant mobility, approximately $18,000\ \text{cm}^2/\text{Vs}$ for this sample. The on-state resistivity is as low as $80\ \text{Ohms}/\text{square}$.

Figure 3b shows the mobility of a graphene FET on SiO_2 as a function of temperature for a carrier concentration of $10^{11}\ \text{cm}^{-2}$.¹¹ The experimentally determined mobility is roughly independent of temperature at low temperature and is limited by disorder. The disorder in mechanically exfoliated graphene on SiO_2 appears to be primarily due to charges trapped at the surface of the SiO_2 or adsorbed on the graphene.^{11,12,40–42} Other possible scattering mechanisms include point defects^{43–45} (though expected to be rare in graphene exfoliated from high-quality graphite crystals), substrate-induced corrugations^{12,27,29} (which may explain the sublinear $\sigma(V_g)$ behavior observed in many devices),^{12,41,42} or weak neutral impurities.⁴⁶ Charged impurity scattering^{11,40,47–49} gives rise to the

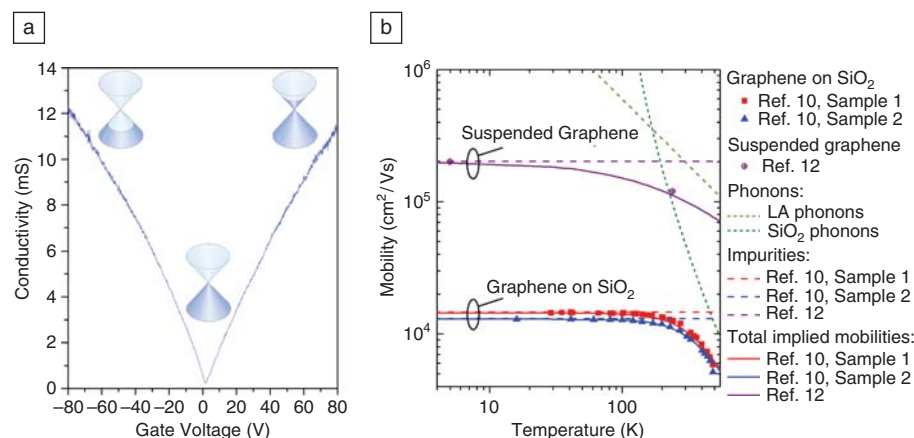


Figure 3. (a) Conductivity as a function of gate voltage for a graphene field-effect transistor on SiO_2 substrate (data courtesy M.S. Fuhrer³⁹). The upright and inverted cones represent the valence and conduction band structure, and the shading indicates the filling of electronic states. (b) Mobility as a function of temperature for graphene on SiO_2 at a carrier density of $10^{11}\ \text{cm}^{-2}$ (blue-filled triangles and red-filled squares);¹¹ suspended graphene at a similar carrier density of $2 \times 10^{11}\ \text{cm}^{-2}$ (open purple circles;⁵⁵ similar values are reported in Reference 56). Blue, red, and purple dashed lines show the contribution from impurities for each sample. The gold dashed line shows the contribution from the longitudinal acoustic (LA) phonons of graphene. The green dashed line shows the contribution from remote interfacial phonon scattering due to the polar optical phonons of the SiO_2 substrate (not applicable to the suspended sample). Solid blue, red, and purple lines show the total contribution from impurities and phonons (graphene LA phonons and SiO_2 optical phonons for graphene on SiO_2 ; graphene LA phonons only for suspended graphene). Note that contributions to mobility are added inversely.

linear $\sigma(V_g)$ observed in graphene on SiO₂ (see Figure 3a) and also explains the magnitude of the minimum conductivity: the random charged impurity potential creates puddles of electrons and holes in nominally charge-neutral graphene,⁴⁸ leading to a finite minimum conductivity.^{4,40,50} Increasing the number of charged impurities decreases the mobility but increases the residual carrier density in the puddles. The result is that the minimum conductivity value is only weakly dependent on disorder and is, on order, a few times the quantum of conductance ($G_0 = 2e^2/h = 7.7 \times 10^{-5}$ S, where e is the elementary charge).

Graphene's mobility begins to show strong temperature dependence near room temperature (see Figure 3b).^{11,12} Surprisingly, this temperature dependence is dominated not by the phonons of graphene itself, but instead by remote interfacial phonon (RIP) scattering from the optical phonons of the SiO₂ substrate.^{51,52} RIP scattering limits the mobility of graphene on SiO₂ to ~40,000 cm²/Vs at room temperature.¹¹ Graphene's longitudinal acoustic phonons give a much weaker contribution,^{11,53} limiting the mobility to ~200,000 cm²/Vs at room temperature at a carrier density of 10^{11} cm⁻². The phonon-limited mobility of graphene on SiO₂ compares favorably to that of InAs and InSb high elec-

tron mobility transistors, for which the highest mobilities achieved in actual devices are ~30,000–40,000 cm²/Vs.⁵⁴ The on/off resistivity ratio of graphene FETs is only ~100:1 in the best devices, but this is suitable for analog device applications.

Removing the SiO₂ substrate removes RIP scattering and also greatly reduces the charged impurity scattering, presumably by eliminating the influence of trapped charges in the SiO₂. Suspended graphene devices, free from the SiO₂ substrate, have shown mobilities as high as 250,000 cm²/Vs at low temperature^{13,55,56} and 120,000 cm²/Vs at 240 K.⁵⁵

Because it is a gapless semiconductor, graphene cannot be directly used for digital electronics (see subsection *Bandgap Engineering in Graphene*). On the other hand, one can take advantage of its ambipolar transport characteristic to make analog devices such as frequency multipliers, high-frequency mixers, zero-volt detectors, and radio receivers.⁵⁷ IBM researchers have recently demonstrated operation of a high-frequency graphene FET, with a cut-off frequency as high as 100 GHz.⁵⁸

Bandgap Engineering in Graphene

Bandgap creation and engineering is crucial for realization of graphene's potential as an electronic material that supplements or replaces silicon. A number of

different approaches have been proposed. Here we focus on three different approaches that have been experimentally realized.

Perhaps the most natural approach to bandgap creation is through quantum confinement of charges in graphene nanoribbons (GNRs).⁵⁹ A GNR is expected to have a bandgap E_g that scales inversely with width (i.e., $E_g = \Delta_0/N_a$), where Δ_0 is an "intrinsic" energy gap, and N_a is the number of atoms across the GNR width. Theoretical calculations⁶⁰ predict that Δ_0 depends on the edge type (armchair versus zigzag, see Figure 4a and 4b), with an additional rapid dependence on N_a with period 3 in the case of armchair nanoribbons. Energy gaps of several hundred meV are expected for widths in the few nanometer range for ideal armchair GNRs, whereas zigzag GNRs may exhibit ferromagnetic metallic edge states.⁶¹

GNRs have been fabricated using a variety of methods, including (1) standard electron beam lithography and etching; (2) chemical exfoliation of graphite, followed by sonication in special surfactants and centrifugation to remove thicker layers; and (3) lithographically or chemically unzipping carbon nanotubes.^{62,63} In transport experiments on lithographically defined^{64,65} and chemically derived GNRs,⁶⁶ a gap has been reported, and the

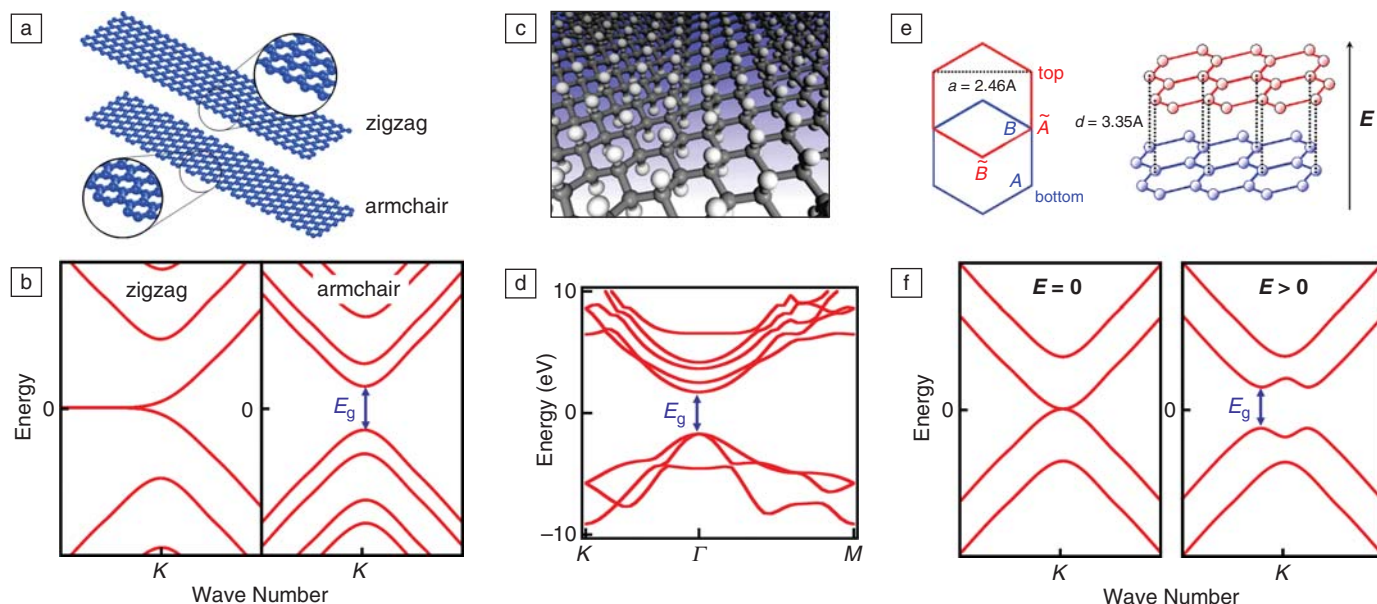


Figure 4. Strategies for opening a bandgap in graphene. (a) Atomic structure of graphene nanoribbons with zigzag and armchair edges (courtesy of M. Bockrath). (b) Schematic band structure of zigzag and armchair graphene nanoribbons. The armchair nanoribbon shows an energy gap that is inversely proportional to width. The zigzag ribbon shows states at zero energy that are localized at the edges of the ribbon. Detailed calculations show that these states may be spin-polarized.⁶¹ (c) Atomic structure of graphene. Grey atoms are carbon, white are hydrogen. (Reprinted with permission from Reference 79. ©2007, American Physical Society.) (d) Band structure of graphene.⁷⁹ K , Γ , and M represent high-symmetry points in the hexagonal Brillouin zone (courtesy of J. Sofo). (e) Atomic structure of Bernal-stacked bilayer graphene. (f) Band structure of Bernal-stacked bilayer graphene without (left) and with (right) perpendicular electric field E .

narrowest GNRs have on/off ratios of $>10^6$ at room temperature.^{66,67} There is considerable debate over how the observed “transport gap” relates to the energy gap (gap in the electronic spectrum), given that transport experiments are also influenced by localization effects due to the disordered edges, defects, and/or impurities.^{68,69} Future experiments will be necessary to clarify and optimize the nature and magnitude of transport gaps in GNRs.

Ideally, the result of graphene electronics research would be “designer” GNRs with controlled, crystallographically oriented edges that enable customization of their electronic properties. For instance, a 5-nm-wide ribbon may display metallic, semiconducting, or even ferromagnetic behavior, depending on its edge orientation. Recently, it was demonstrated that at elevated temperatures, Ni or Fe nanoparticles etch thin graphite and graphene sheets,^{70–72} leaving trenches at abrupt angles, suggesting that they move along specific crystallographic directions. This surprising discovery, combined with efforts to functionalize or passivate the edges, might enable ribbons with tailored electronic properties.

Chemical modification of graphene (e.g., by reaction with atomic hydrogen^{73,74} or through solution chemistry^{75,76}) also offers a promising route for bandgap engineering, with the advantage of being scalable and inexpensive. Recently, graphene was found to display semiconducting behavior after exposure to a hydrogen plasma (Figure 4d).^{73,74} During hydrogenation, each hydrogen atom removes a π electron from graphene via a sp^2 -to- sp^3 transformation of the carbon atom bonding pattern. The fully hydrogenated compound, graphane, is predicted to be a semiconductor with a 3.5 eV energy gap.^{77–79} Graphane is stable at room temperature, exhibiting semiconducting transport properties. Remarkably, upon annealing at 450°C, graphane reverts to the gapless graphene state, and metallic conduction (including even the quantum Hall effect) can be recovered.⁷³

The discovery of graphane opens up a new front for chemical bandgap engineering and synthesis of novel graphene-related materials. In general, one can expect an intricate interplay between electronic structure, hydrogen ordering,^{80,81} and corrugation of the graphene sheet, resulting in higher stability of some of the configurations/coverages than others. In fact, we expect an entire family of stable macromolecules bridging graphene and graphane.

So far most attention has focused on single-layer graphene. Recently, however,

bilayer graphene has increasingly shared the spotlight (see Figure 4e). The band structure of bilayer graphene is unusual and distinct from single-layer graphene: bilayer graphene has massive (parabolic) valence and conduction bands but remains gapless—the conduction and valence bands touch at the charge neutrality point^{82,83} (see Figure 4f [left]). However, when an electric field is applied perpendicular to bilayer graphene, a bandgap opens at the charge-neutrality point, and the valence and conduction bands adopt a “Mexican hat” shape (see Figure 4f [right]).^{84,85} The electric field-induced gap has recently been measured in photoemission⁸⁶ and optical^{87,88} experiments to be as large as ~200 mV. Transport measurements in gapped bilayer graphene show insulating behavior characteristic of disordered semiconductors, probably indicating that the disorder strength is still larger than the energy gap in current bilayer graphene samples.⁸⁹

Beyond CMOS

A number of research efforts seeking electronic technologies “beyond CMOS” are focused on the realization of computing devices based on state variables other than charge. An example is “spintronics,” in which information is stored and manipulated in the electron’s spin.⁹⁰ Because of the low atomic number of carbon and the predominance of the spin-zero carbon-12 nucleus (making up 99% of naturally occurring carbon), carbon atoms have weak spin-orbit and hyperfine couplings, hence a potential for very long spin lifetimes. When combined with its very large current-carrying capacity, these attributes make graphene an attractive candidate for spin-conserving, conducting elements in spintronic circuits. Experimental studies of spin lifetimes and spin propagation in graphene are promising but are still at an early stage^{91–94} and not yet completely understood. In particular, the measured spin lifetime is much shorter than expected,⁹⁴ possibly due to disorder or edge chemistry.

Looking further into the future, graphene is also a promising material for pseudospintronics. Pseudospintronics refers to the storage and manipulation of any two valued quantum degree-of-freedom other than spin.^{95,96} Unlike spintronics, pseudospintronics has so far remained almost exclusively a theoretical notion. The most attractive degree of freedom for pseudospintronics appears to be the *which-layer* degree of freedom of a two-layer two-dimensional electron system, in which separate contacts to the individual layers provide a ready source of half-

metallic electronic reservoirs. In the case of graphene, there are at least three distinct types of two-layer systems: AB stacked bilayers, which are readily obtained by mechanical exfoliation of graphite, rotated layers, which form in epitaxial graphene grown on SiC substrates, and two isolated graphene layers, which are separated by a dielectric. In all of these cases, an electric potential difference between top and bottom layers acts like an effective magnetic field that favors one pseudospin state over the other, thus providing a platform for single-particle pseudospintronic devices.⁹⁶ Even more enticing, it now may be possible to create two-layer graphene systems that exhibit pseudospin ferromagnetism. Nearly neutral AB bilayers, for example, could be Ising-like pseudospin ferromagnets, in which charge is spontaneously transferred between layers.⁹⁷ The electronically isolated bilayer systems could be XY-like pseudospin ferromagnets, in which phase coherence is spontaneously established between separate layers. Both types of pseudospin ferromagnetism would⁹⁸ lead to spectacular electrical effects in separately contacted bilayers.

Spontaneous interlayer phase coherence is a type of condensed matter order that has been imagined for many years but realized so far only in semiconductor bilayers and only at low temperatures and in extremely strong magnetic fields. Spontaneous coherence is associated with exciton condensation and is closely analogous to superfluidity due to ^3He - ^3He pair formation in liquid ^3He . It has been predicted⁹⁹ that spontaneous phase coherence might occur in electrically isolated graphene bilayers that have high densities of electrons and holes in opposite layers and a layer separation that is comparable to or smaller than the distance between carriers within a layer. Given the disorder present in graphene samples on substrates, realization of this exotic state appears to require electron and hole densities $\sim 10^{13} \text{ cm}^{-2}$ and layer separations of not more than a few nm. Progress is being made in engineering circumstances favorable for this form of pseudospin ferromagnetism.¹⁰⁰

Other Applications of Graphene

In addition to being an excellent conductor with fascinating electrical properties, graphene is also nature’s thinnest elastic membrane, opening the door for new electromechanical applications. Graphene can sustain $>20\%$ strain without breaking,²³ and the strain dependence of its conductivity can be exploited to enable piezoelectric materials,⁸ strain sensors, or flexible electronics. Despite being only one atomic layer thick, graphene is also an

amazingly strong material, with a Young's modulus of ~ 1 TPa^{23,101} and a breaking strength of ~ 130 GPa.²³ These attributes make graphene an ideal candidate for nanoelectromechanical applications, such as mass detection with unparalleled sensitivity. Nanomechanical resonators based on freestanding graphene membranes have been demonstrated¹⁰² and may lead to ultrasensitive position, force, and mass sensors.

Graphene is also an optically transparent membrane. Interestingly, the optical transmittance of freestanding single-layer neutral graphene is independent of frequency and other material constants and is given by $(1 - \pi\alpha) \approx 0.97$, where

$$\alpha \equiv \frac{e^2}{\hbar c} \approx \frac{1}{137} \quad (1)$$

is the fine structure constant, with c being the speed of light.^{35–37} Thus graphene is a transparent, chemically stable, highly conducting thin film, with numerous potential applications in solar cells, displays, and other optoelectronic devices. A particularly compelling aspect of this application is that it does not require single or bilayer graphene: 90% transparent thin films have been demonstrated by spray painting thin graphite sheets that are chemically exfoliated and suspended in dimethylformamide solution,¹⁰³ so that mass production of such thin films at relatively low cost appears already feasible.

A third emerging application of graphene is in chemical and biological sensors, enabled by graphene's extreme sensitivity to its electromagnetic environment. Conceptually, an adsorbate molecule can transfer electrical charge to graphene, hence changing its electrochemical potential and resistance. Graphene sensors that can detect single molecule events have been reported¹⁰⁴ and will undoubtedly be explored for future sensing technologies.

Graphene also has potential as an energy storage material, either in batteries or electrochemical supercapacitors. Graphitic carbon is already the most commonly used material for the negative electrode of lithium ion batteries,¹⁰⁵ and composite materials containing graphitic carbon can improve the conductivity and structural stability of positive and negative electrode materials.^{106–108} Graphene is now being explored directly for its potential in supercapacitors, which take advantage of its enormous surface area per unit mass. Graphene-based systems already have performance characteristics comparable to those of ultra-capacitor systems in current use,¹⁰⁹ and there is hope that substantial further progress will be possible.

Conclusions

Graphene is a fundamentally new electronic material, whose electrons are strictly confined to an atomically thin two-dimensional plane and exhibit properties mimicking those of ultrarelativistic particles. In this review, we have attempted to provide a brief snapshot of this extremely rapidly moving field. Graphene is immediately applicable to high-speed analog electronic devices and transparent, flexible, highly conducting thin films. A significant portion of current research efforts in graphene focuses on generating and tuning a bandgap through nanostructuring, chemical modification, or, in the case of bilayer graphene, by application of a perpendicular electric field. Gapped graphene could enable graphene-based CMOS logic and may be useful in other applications, such as optoelectronics, where a tunable direct bandgap is desirable. Graphene is also being studied for applications beyond CMOS, including spintronics and pseudospintronics. New exotic electronic states, such as excitonic superfluid in decoupled graphene bilayers, may be used to realize low dissipation computing devices. Graphene research is proceeding rapidly, with new results announced daily. Its extraordinary materials properties appear certain to enable applications not yet anticipated.

Acknowledgments


M.S.F. acknowledges support by the U.S. ONR MURI program, an NRI-MRSEC supplemental grant, NSF-UMD-MRSEC grant DMR 05-20471, and NSF-DMR grant 08-04976, and U.S. Department of Energy grant DESL0001160. C.N.L. acknowledges support by NSF CAREER DMR/0748910, NSF/ECCS 0926056, ONR N00014-09-1-0724, and UC Lab Fees Research Program 09-LR-06-117702-BASD. A.H.M. acknowledges support from SWAN, the NSF-NRI program, and the Welch Foundation.

References

1. C. Oshima, A. Nagashima, *J. Phys.* **9**, 1 (1997).
2. K.S. Novoselov, A.K. Geim, S.V. Morozov, D. Jiang, Y. Zhang, S.V. Dubonos, I.V. Grigorieva, A.A. Firsov, *Science* **306**, 666 (2004).
3. K.S. Novoselov, D. Jiang, F. Schedin, T.J. Booth, V.V. Khotkevich, S.V. Morozov, A.K. Geim, *PNAS* **102**, 10451 (2005).
4. K.S. Novoselov, A.K. Geim, S.V. Morozov, D. Jiang, M.I. Katsnelson, I.V. Grigorieva, S.V. Dubonos, A.A. Firsov, *Nature* **438**, 197 (2005).
5. Y.B. Zhang, Y.W. Tan, H.L. Stormer, P. Kim, *Nature* **438**, 201 (2005).
6. V.P. Gusynin, S.G. Sharapov, *Phys. Rev. Lett.* **95**, 146801 (2005).
7. C. Berger, Z.M. Song, X.B. Li, X.S. Wu, N. Brown, C. Naud, D. Mayo, T.B. Li, J. Hass, A.N. Marchenkov, E.H. Conrad, P.N. First, W.A. de Heer, *Science* **312**, 1191 (2006).

8. K.S. Kim, Y. Zhao, H. Jang, S.Y. Lee, J.M. Kim, J.H. Ahn, P. Kim, J.Y. Choi, B.H. Hong, *Nature* **457**, 706 (2009).
9. X.S. Li, W.W. Cai, J.H. An, S. Kim, J. Nah, D.X. Yang, R. Piner, A. Velamakanni, I. Jung, E. Tutuc, S.K. Banerjee, L. Colombo, R.S. Ruoff, *Science* **324**, 1312 (2009).
10. A. Reina, X.T. Jia, J. Ho, D. Nezich, H.B. Son, V. Bulovic, M.S. Dresselhaus, J. Kong, *Nano Lett.* **9**, 30 (2009).
11. J.H. Chen, C. Jang, S.D. Xiao, M. Ishigami, M.S. Fuhrer, *Nat. Nanotechnol.* **3**, 206 (2008).
12. S.V. Morozov, K.S. Novoselov, M.I. Katsnelson, F. Schedin, D.C. Elias, J.A. Jaszczak, A.K. Geim, *Phys. Rev. Lett.* **100**, 016602 (2008).
13. K.I. Bolotin, K.J. Sikes, Z. Jiang, M. Klima, G. Fudenberg, J. Hone, P. Kim, H.L. Stormer, *Solid State Commun.* **146**, 351 (2008).
14. A.A. Balandin, S. Ghosh, W. Bao, I. Calizo, D. Teweldebrhan, F. Miao, C.N. Lau, *Nano Lett.* **8**, 902 (2008).
15. B. Standley, W. Bao, H. Zhang, J. Bruck, C.N. Lau, M. Bockrath, *Nano Lett.* **8**, 3345 (2008).
16. J. Moser, A. Barreiro, A. Bachtold, *Appl. Phys. Lett.* **91**, 163513 (2007).
17. P.R. Wallace, *Phys. Rev.* **71**, 622 (1947).
18. T. Ando, T. Nakanishi, R. Saito, *J. Phys. Soc. Jpn.* **67**, 2857 (1998).
19. P.L. McEuen, M. Bockrath, D.H. Cobden, Y.G. Yoon, S.G. Louie, *Phys. Rev. Lett.* **83**, 5098 (1999).
20. A. Bachtold, M.S. Fuhrer, S. Plyasunov, M. Forero, E.H. Anderson, A. Zettl, P.L. McEuen, *Phys. Rev. Lett.* **84**, 6082 (2000).
21. M. Purewal, B.H. Hong, A. Ravi, B. Chandra, J. Hone, P. Kim, *Phys. Rev. Lett.* **98**, 186808 (2007).
22. A.B. Fowler, F.F. Fang, W.E. Howard, P.J. Stiles, *J. Phys. Soc. Jpn.* **S 21**, 331 (1966).
23. C. Lee, X.D. Wei, J.W. Kysar, J. Hone, *Science* **321**, 385 (2008).
24. J.S. Bunch, S.S. Verbridge, J.S. Alden, A.M. van der Zande, J.M. Parpia, H.G. Craighead, P.L. McEuen, *Nano Lett.* **8**, 2458 (2008).
25. W. Bao, F. Miao, Z. Chen, H. Zhang, W. Jang, C. Dames, C.N. Lau, *Nat. Nanotechnol.* **4**, 562 (2009).
26. E.-A. Kim, A.H. Castro Neto, *Europhys. Lett.* **84**, 57007 (2008).
27. M.I. Katsnelson, A.K. Geim, *Philos. Trans. R. Soc. A* **366**, 195 (2008).
28. F. Guinea, B. Horowitz, P. Le Doussal, *Phys. Rev. B* **77**, 205421 (2008).
29. F. Guinea, M.I. Katsnelson, M.A.H. Vozmediano, *Phys. Rev. B* **77**, 075422 (2008).
30. A.L.V. de Parga, F. Calleja, B. Borca, M.C.G. Passeggi, J.J. Hinarejos, F. Guinea, R. Miranda, *Phys. Rev. Lett.* **100**, 056807 (2008).
31. V.M. Pereira, A.H. Castro Neto, (2008), arXiv:0810.4539v1.
32. Z. Chen, W. Jang, W. Bao, C.N. Lau, C. Dames, *Appl. Phys. Lett.* **95**, 161910 (2009).
33. A.C. Ferrari, J.C. Meyer, V. Scardaci, C. Casiraghi, M. Lazzeri, F. Mauri, S. Piscanec, D. Jiang, K.S. Novoselov, S. Roth, A.K. Geim, *Phys. Rev. Lett.* **97**, 187401 (2006).
34. P. Blake, E.W. Hill, A.H.C. Neto, K.S. Novoselov, D. Jiang, R. Yang, T.J. Booth, A.K. Geim, *Appl. Phys. Lett.* **91** (2007).
35. A.B. Kuzmenko, E. van Heumen, F. Carbone, D. van der Marel, *Phys. Rev. Lett.* **100**, 117401 (2008).

36. K.F. Mak, M.Y. Sfeir, W. Yang, L. Chun Hung, J.A. Misewich, T.F. Heinz, *Phys. Rev. Lett.* **101**, 196405 (2008).
37. R.R. Nair, P. Blake, A.N. Grigorenko, K.S. Novoselov, T.J. Booth, T. Stauber, N.M.R. Peres, A.K. Geim, *Science* **320**, 1308 (2008).
38. C. Berger, Z.M. Song, T.B. Li, X.B. Li, A.Y. Ogbazghi, R. Feng, Z.T. Dai, A.N. Marchenkov, E.H. Conrad, P.N. First, W.A. de Heer, *J. Phys. Chem. B* **108**, 19912 (2004).
39. S. Cho, M.S. Fuhrer, *Phys. Rev. B* **77**, 081402 (2008).
40. S. Adam, E.H. Hwang, V.M. Galitski, S. Das Sarma, *PNAS* **104**, 18392 (2007).
41. C. Jang, S. Adam, J.-H. Chen, E.D. Williams, S. Das Sarma, M.S. Fuhrer, *Phys. Rev. Lett.* **101**, 146805 (2008).
42. J.-H. Chen, C. Jang, M. Ishigami, S. Xiao, E.D. Williams, M.S. Fuhrer, *Solid State Commun.* **149**, 1080 (2009).
43. J.-H. Chen, W.G. Cullen, C. Jang, M.S. Fuhrer, E.D. Williams, *Phys. Rev. Lett.* **102**, 236805 (2009).
44. M. Hentschel, F. Guinea, *Phys. Rev. B* **76**, 115407 (2007).
45. T. Stauber, N.M.R. Peres, F. Guinea, *Phys. Rev. B* **76**, 205423 (2007).
46. N.H. Shon, T. Ando, *J. Phys. Soc. Jpn.* **67**, 2421 (1998).
47. T. Ando, *J. Phys. Soc. Jpn.* **75**, 074716 (2006).
48. E.H. Hwang, S. Adam, S. Das Sarma, *Phys. Rev. Lett.* **98**, 186806 (2007).
49. K. Nomura, A.H. MacDonald, *Phys. Rev. Lett.* **98**, 076602 (2007).
50. E. Rossi, S. Adam, S. Das Sarma, *Phys. Rev. B* **79**, 245423 (2009).
51. K. Hess, P. Vogl, *Solid State Commun.* **30**, 807 (1979).
52. S. Fratini, F. Guinea, *Phys. Rev. B* **77**, 195415 (2008).
53. E.H. Hwang, S. Das Sarma, *Phys. Rev. B* **77**, 115449 (2008).
54. B.R. Bennett, R. Magno, J.B. Boos, W. Kruppa, M.G. Ancona, *Solid-State Electron.* **49**, 1875 (2005).
55. K.I. Bolotin, K.J. Sikes, J. Hone, H.L. Stormer, P. Kim, *Phys. Rev. Lett.* **101**, 096802 (2008).
56. X. Du, I. Skachko, A. Barker, E.Y. Andrei, *Nat. Nanotechnol.* **3**, 491 (2008).
57. H. Wang, D. Nezich, J. Kong, T. Palacios, *IEEE Electron Device Lett.* **30**, 547 (2009).
58. Y.-M. Lin, C. Dimitrakopoulos, K.A. Jenkins, D.B. Farmer, H.-Y. Chiu, A. Grill, Ph. Avouris, *Science* **327**, 662 (2010).
59. K. Nakata, M. Fujita, G. Dresselhaus, M.S. Dresselhaus, *Phys. Rev. B* **54**, 17954 (1996).
60. Y.W. Son, M.L. Cohen, S.G. Louie, *Phys. Rev. Lett.* **97**, 216803 (2006).
61. Y.W. Son, M.L. Cohen, S.G. Louie, *Nature* **444**, 347 (2006).
62. L.Y. Jiao, L. Zhang, X.R. Wang, G. Diankov, H.J. Dai, *Nature* **458**, 877 (2009).
63. D.V. Kosynkin, A.L. Higginbotham, A. Sinitskii, J.R. Lomeda, A. Dimiev, B.K. Price, J.M. Tour, *Nature* **458**, 872 (2009).
64. Z.H. Chen, Y.M. Lin, M.J. Rooks, P. Avouris, *Phys. E* **40**, 228 (2007).
65. M.Y. Han, B. Ozyilmaz, Y.B. Zhang, P. Kim, *Phys. Rev. Lett.* **98**, 206805 (2007).
66. X.L. Li, X.R. Wang, L. Zhang, S.W. Lee, H.J. Dai, *Science* **319**, 1229 (2008).
67. X. Wang, Y. Ouyang, X. Li, H. Wang, J. Guo, H. Dai, *Phys. Rev. Lett.* **100**, 206803 (2008).
68. F. Sols, F. Guinea, A.H.C. Neto, *Phys. Rev. Lett.* **99**, 166803 (2007).
69. K. Todd, H.T. Chou, S. Amasha, D. Goldhaber-Gordon, *Nano Lett.* **9**, 416 (2009).
70. L.C. Campos, V.R. Manfrinato, J.D. Sanchez-Yamagishi, J. Kong, P. Jarillo-Herrero, *Nano Lett.* **9**, 2600 (2009).
71. L. Ci, Z. Xu, L. Wang, W. Gao, F. Ding, K. Kelly, B. Yakobson, P. Ajayan, *Nano Res.* **1**, 116 (2008).
72. S.S. Datta, D.R. Strachan, S.M. Khamis, A.T.C. Johnson, *Nano Lett.* **8**, 1912 (2008).
73. D.C. Elias, R.R. Nair, T.M.G. Mohiuddin, S.V. Morozov, P. Blake, M.P. Halsall, A.C. Ferrari, D.W. Boukhvalov, M.I. Katsnelson, A.K. Geim, K.S. Novoselov, *Science* **323**, 610 (2009).
74. S. Ryu, M.Y. Han, J. Maultzsch, T.F. Heinz, P. Kim, M.L. Steigerwald, L.E. Brus, *Nano Lett.* **8**, 4597 (2008).
75. J.R. Lomeda, C.D. Doyle, D.V. Kosynkin, W.-H. Hwang, J.M. Tour, *J. Am. Chem. Soc.* **130**, 16201 (2008).
76. E. Bekyarova, M.E. Itkis, P. Ramesh, C. Berger, M. Sprinkle, W.A. de Heer, R.C. Haddon, *J. Am. Chem. Soc.* **131**, 1336 (2009).
77. D.W. Boukhvalov, M.I. Katsnelson, A.I. Lichtenstein, *Phys. Rev. B* **77**, 035427 (2008).
78. K. Novoselov, *Phys. World* **27** (2009).
79. J.O. Sofo, A.S. Chaudhari, G.D. Barber, *Phys. Rev. B* **75**, 153401 (2007).
80. A.V. Shytov, D.A. Abanin, L.S. Levitov, *Phys. Rev. Lett.* **103**, 016806 (2009).
81. L.A. Chernozatonskii, P.B. Sorokin, J.W. Bruning, *Appl. Phys. Lett.* **91**, 183103 (2007).
82. E. McCann, V.I. Fal'ko, *Phys. Rev. Lett.* **96**, 086805 (2006).
83. K.S. Novoselov, E. McCann, S.V. Morozov, V.I. Fal'ko, M.I. Katsnelson, U. Zeitler, D. Jiang, F. Schedin, A.K. Geim, *Nature Phys.* **2**, 177 (2006).
84. E.V. Castro, K.S. Novoselov, S.V. Morozov, N.M.R. Peres, J. Dos Santos, J. Nilsson, F. Guinea, A.K. Geim, A.H. Castro Neto, *Phys. Rev. Lett.* **99**, 216802 (2007).
85. E. McCann, *Phys. Rev. B* **74**, 161403 (2006).
86. T. Ohta, A. Bostwick, T. Seyller, K. Horn, E. Rotenberg, *Science* **313**, 951 (2006).
87. K.F. Mak, C.H. Lui, J. Shan, T.F. Heinz, *Phys. Rev. Lett.* **102**, 256405 (2009).
88. Y.B. Zhang, T.T. Tang, C. Girit, Z. Hao, M.C. Martin, A. Zettl, M.F. Crommie, Y.R. Shen, F. Wang, *Nature* **459**, 820 (2009).
89. J.B. Oostinga, H.B. Heersche, X.L. Liu, A.F. Morpurgo, L.M.K. Vandersypen, *Nat. Mater.* **7**, 151 (2008).
90. I. Zutic, J. Fabian, S.D. Sarma, *Rev. Mod. Phys.* **76**, 323 (2004).
91. S. Cho, Y.-F. Chen, M.S. Fuhrer, *Appl. Phys. Lett.* **91**, 123105 (2007).
92. W. Han, K. Pi, W. Bao, K.M. McCreary, Y. Li, W.H. Wang, C.N. Lau, R.K. Kawakami, *Appl. Phys. Lett.* **94**, 222109 (2009).
93. N. Tombros, C. Jozsa, M. Popinciuc, H.T. Jonkman, B.J. van Wees, *Nature* **448**, 571 (2007).
94. N. Tombros, S. Tanabe, A. Veligura, C. Jozsa, M. Popinciuc, H.T. Jonkman, B.J. van Wees, *Phys. Rev. Lett.* **101**, 046601 (2008).
95. S.H. Abedinpour, M. Polini, A.H. MacDonald, B. Tanatar, M.P. Tosi, G. Vignale, *Phys. Rev. Lett.* **99**, 206802 (2007).
96. P. San-Jose, E. Prada, E. McCann, H. Schomerus, *Phys. Rev. Lett.* **102**, 247204 (2009).
97. H. Min, G. Borghi, M. Polini, A.H. MacDonald, *Phys. Rev. B* **77**, 041407 (2008).
98. J.J. Su, A.H. MacDonald, *Nat. Phys.* **4**, 799 (2008).
99. H.K. Min, R. Bistritzer, J.J. Su, A.H. MacDonald, *Phys. Rev. B* **78**, 121401 (2008).
100. E. Tutuc, personal communication.
101. I.W. Frank, D.M. Tanenbaum, A.M. Van der Zande, P.L. McEuen, *J. Vac. Sci. Technol. B* **25**, 2558 (2007).
102. J.S. Bunch, A.M. van der Zande, S.S. Verbridge, I.W. Frank, D.M. Tanenbaum, J.M. Parpia, H.G. Craighead, P.L. McEuen, *Science* **315**, 490 (2007).
103. P. Blake, P.D. Brimicombe, R.R. Nair, T.J. Booth, D. Jiang, F. Schedin, L.A. Ponomarenko, S.V. Morozov, H.F. Gleeson, E.W. Hill, A.K. Geim, K.S. Novoselov, *Nano Lett.* **8**, 1704 (2008).
104. F. Schedin, K.S. Novoselov, S.V. Morozov, D. Jiang, E.H. Hill, P. Blake, A.K. Geim, *Nat. Mater.* **6**, 652 (2007).
105. M. Winter, J.O. Besenhard, M.E. Spahr, P. Novak, *Adv. Mater.* **10**, 725 (1998).
106. C.R. Sides, F. Croce, V.Y. Young, C.R. Martin, B. Scrosati, *Electrochem. Solid State Lett.* **8**, A484 (2005).
107. H. Zhang, G.P. Cao, Z.Y. Wang, Y.S. Yang, Z.J. Shi, Z.N. Gu, *Nano Lett.* **8**, 2664 (2008).
108. W.M. Zhang, J.S. Hu, Y.G. Guo, S.F. Zheng, L.S. Zhong, W.G. Song, L.J. Wan, *Adv. Mater.* **20**, 1160 (2008).
109. M.D. Stoller, S.J. Park, Y.W. Zhu, J.H. An, R.S. Ruoff, *Nano Lett.* **8**, 3498 (2008). □




IWN2010
International Workshop on Nitride Semiconductors
www.IWN2010.org

International Workshop on Nitride Semiconductors

September 19-24, 2010 • Marriott Tampa Waterside Hotel & Marina, Tampa, Florida, USA

CALL FOR PAPERS

Abstract Submission Ends **June 10, 2010**





Stacks of apps.

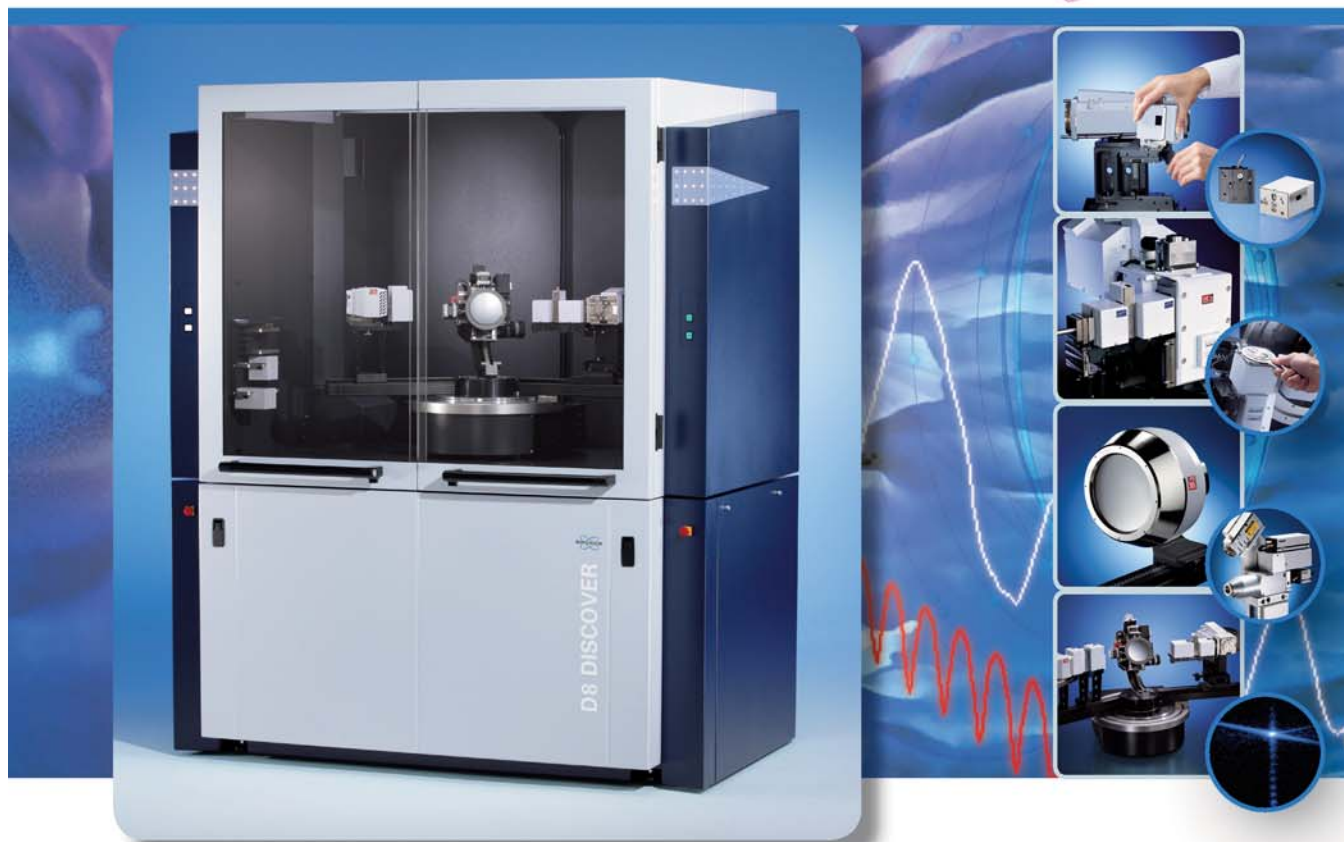
Solartron Analytical provides a range of solutions that enable researchers to measure the electrical properties of materials. Testing at both high and low temperatures is simplified using the tightly integrated temperature control capability, while our comprehensive data acquisition / materials analysis software completes the picture and helps build a winning hand for your research.

See how our products are used in **your** application by searching our extensive online applications reference library, or book a demo or sales call, via our website at: www.solartronanalytical.com/stacksofapps



US: Tel: 1-865-425-1360
 UK: Tel: +44 (0)1252 556800
solartron.info@ametec.com

Bruker AXS



The new D8 DISCOVER with DAVINCI

● Move up to the next dimension in X-ray diffraction

- DAVINCI.SNAP-LOCK & DAVINCI.MODE: alignment-free optics change with real-time component recognition
- TURBO-X-RAY-SOURCE: boost intensity for point, line or micro focus applications
- TWIST-TUBE: fast and easy switching from line to point focus
- VÅNTEC-500 detector: add the extra dimension of XRD²
- PATHFINDER optics: motorized switching between high-resolution and high-intensity beam paths

www.bruker-axs.com

think forward

XRD